HHS Public Access

Author manuscript

*Toxicol Appl Pharmacol*. Author manuscript; available in PMC 2016 January 01.

Published in final edited form as:

*Toxicol Appl Pharmacol*. 2015 January 1; 282(1): 100–107. doi:10.1016/j.taap.2014.10.019.

# High level of oxygen treatment causes cardiotoxicity with arrhythmias and redox modulation

**Kalyan C. Chapalamadugu**[1,†], **Siva K. Panguluri**[1,†], **Eric S. Bennett**[2], **Narasaiah Kolliputi**[3], and **Srinivas M. Tipparaju**[1,*]

[1]Department of Pharmaceutical Sciences, College of Pharmacy, University of South Florida, Tampa, Florida, USA

[2]Department of Molecular Pharmacology and Physiology, Morsani College of Medicine, University of South Florida, Tampa, Florida, USA

[3]Division of Allergy and Immunology, Department of Internal Medicine, Morsani College of Medicine, University of South Florida, Tampa, Florida, USA

## Abstract

Hyperoxia exposure in mice leads to cardiac hypertrophy and voltage-gated potassium (Kv) channel remodeling. Because redox balance of pyridine nucleotides affects Kv function and hyperoxia alters cellular redox potential, we hypothesized that hyperoxia exposure leads to cardiac ion channel disturbances and redox changes resulting in arrhythmias. In the present study, we investigated the electrical changes and redox abnormalities caused by 72h hyperoxia treatment in mice. Cardiac repolarization changes were assessed by acquiring electrocardiogram (ECG) and cardiac action potentials (AP). Biochemical assays were employed to identify the pyridine nucleotide changes, Kv1.5 expression and myocardial injury. Hyperoxia treatment caused marked bradycardia, arrhythmia and significantly prolonged (ms) the, RR (186.2 ±10.7 *vs.* 146.4±6.2), PR (46.8±3.1 *vs.* 39.3±1.6), QRS (10.8±0.6 *vs.* 8.5±0.2), QTc (57.1±3.5 *vs.* 40±1.4) and JT (13.4±2.1 *vs.* 7.0±0.5) intervals, when compared with normoxia group. Hyperoxia treatment also induced significant increase in cardiac action potential duration (APD) (ex- $APD_{90}$; 73.8±9.5 *vs.* 50.9±3.1 ms) and elevated levels of serum markers of myocardial injury; cardiac troponin I (TnI) and lactate dehydrogenase (LDH). Hyperoxia exposure altered cardiac levels of mRNA/protein expression of; Kv1.5, Kvβ subunits and SiRT1, and increased ratios of reduced pyridine nucleotides (NADH/NAD & NADPH/NADP). Inhibition of SiRT1 in H9C2 cells using Splitomicin resulted in decreased SiRT1 and Kv1.5 expression, suggesting that SiRT1 may



*Corresponding Author: Srinivas Tipparaju, MPharm, PhD, Departmental Pharmaceutical Sciences, University of South Florida, College of Pharmacy, 12901 Bruce B. Downs Blvd. Suite# MDC4031, Tampa, FL, USA, Phone: 813-974-7195, stippara@health.usf.edu.

†Authors with equal contribution.



**Conflict of interest statement:**

The authors have no conflict of interests. No disclosures.

mediate Kv1.5 downregulation. In conclusion, the cardiotoxic effects of hyperoxia exposure involve ion channel disturbances and redox changes resulting in arrhythmias.

### Keywords

hyperoxia; ECG; heart; action potential; redox; Kvβ; potassium channel

## Introduction

Earlier studies show that hyperoxia causes dysfunctional lung and compromised pulmonary functioning, which increases workload on the heart triggering cardiac remodeling (44, 48). Hyperoxia exposure results in significant hemodynamic changes including decreased stroke volume and cardiac output (16, 39, 45). We recently showed that 3 days of hyperoxia treatment in adult mice results in significant cardiac hypertrophy and marked ion channel disturbances (33), suggesting that prolonged hyperoxia exposure induces profound pathophysiological remodeling in heart. We therefore undertook the present study to provide an in-depth understanding of the cardiotoxic effects of high level of oxygen treatment with respect to arrhythmogenic potential and redox abnormalities.

The ratios of oxidized and reduced pyridine nucleotides is tightly linked to metabolism, and alteration in the levels of pyridine nucleotides leads to changes in redox status. The nucleotide ratios change significantly in cardiac pathologies including hypertrophy and ischemia-reperfusion injury (8, 36). It is also widely recognized that hyperoxia alters redox balance and increases the oxidative stress in multiple tissues (2, 5, 7, 34). Cellular redox status is an important determinant of cardiac function. Pyridine nucleotides that are major intracellular redox modulators regulate the Kv channel activity (3, 22, 24). Given the significant structural and ion channel disturbances reported in hyperoxia treated mouse hearts, we hypothesize that hyperoxia exposure leads to cardiac ion channel disturbances and redox changes resulting in arrhythmias. Therefore, we investigated the arrhythmogenesis in mice exposed to hyperoxia using electrocardiography (ECG) and *ex vivo* approaches. To understand the mechanistic basis of cardiac electrical abnormalities observed in hyperoxia treated mice, we also investigated the expression of Kv1.5, Kvβ's and SiRT1 along with pyridine nucleotide [(NAD(P)H/NAD(P)] levels in the heart. Our results delineate the potential role of SiRT1 and pyridine nucleotides in hyperoxia induced electrical changes that may lead to arrhythmogenesis.

## Materials & Methods

### Animals

C57BL/6 mice were obtained from Jackson Laboratories (Bar Harbor, ME, US). Experimental protocol for use of animals in research was approved by the Institutional Animal Care and Use Committee at the University of South Florida (Tampa, FL, US), which was in accordance with US National Institutes of Health guidelines. Mice (10 week old) were randomly assigned into two groups and exposed to either 100% oxygen (hyperoxia) or room air (normoxia) for 72h, as described previously by Panguluri et al. (2013) (33). All the

mice had continuous access to food and water, *ad libitum*. Body weight of each animal was recorded before and after 72h hyperoxia or normoxia treatment.

## Electrocardiography (ECG)

ECG recordings were obtained on mice anesthetized with isoflurane (1–2%) using surface probes in lead II configuration. ECG's were recorded for total duration of 15 minutes, with 1 minute recordings obtained at 5 minute intervals. Heart rate was measured while ECG signals were obtained. Signal was acquired at 1000 μs rate by using PowerLab system operated with LabChart 7.2 software (AD instruments, UK), and data was analyzed offline using the ECG module of LabChart 7.2 software, as reported elsewhere (4). Intervals (ms) of RR, PR, QRS and JT were measured. QT interval was measured form the start of Q peak to the point where the T wave returns to the isoelectric baseline (TP baseline), and heart rate corrected QT (QTc) interval was obtained using the Bazett's formula ($QTc=QT/RR^{1/2}$).

## Cardiac Action Potentials

Mice were injected with heparin (360 USP units, Sigma-Aldrich, MO) and euthanized with Somnasol™ (pentobarbital, 50mg/kg i.p. body weight). The hearts were mounted on to the langendorff apparatus immediately, and perfused with Krebs-Hanseleit buffer containing (in mM): 119 NaCl, 25 $NaHCO_3$ , 4 KCl, 1 $MgCl_2$, 1.8 $CaCl_2$, 1 $MgCl_2$, 10 glucose and 2 Sodium pyruvate, pH 7.4, that was constantly bubbled with carbogen gas and maintained at 37°C. Perfusion was maintained at a constant flow of ~2.2 ml/min. Hearts were stabilized for 10 min before data acquisition. Action potentials (AP) were acquired under sinus rhythm as reported previously (26). Signal was acquired at 1000 μs rate using an 8 channel PowerLab system run by LabChart 7.2 software (AD instruments, UK). Action potentials were analyzed using LabChart 7.2 software, and AP duration (APD) at 10, 20, 50, 70 and 90% level of repolarization was assessed from the peak amplitude to obtain $APD_{10}$, $APD_{30}$, $APD_{50}$, $APD_{70}$, and $APD_{90}$, respectively.

## Hyperoxia induced lung injury

Lungs from hyperoxia or normoxia exposed mice were harvested from the hilum and lung edema (wet to dry lung weight ratio) was assessed as described previously (15, 25). Briefly, isolated lungs were dry blotted, weighed to obtain wet weight and desiccated overnight at 130°C in vacuum oven. Dry lung weights were then recorded and the ratio of the wet to dry weights was calculated. We also determined the total number of cells in the Bronchoalveolar lavage fluid (BALF) as reported before (15, 25). Bronchoalveolar lavage was performed by infusing sterile PBS into the lungs through a catheter inserted into the trachea after skin incision in the ventral neck region. Cells were pelleted by centrifuging at 400xg for 10 min at 4°C and resuspended in 1 mL PBS. A hematocytometer was used to count the total number of cells in the BALF.

## Biochemical assays

Serum samples collected from hyperoxia or normoxia mice were analyzed for lactate dehydrogenase (LDH) and cardiac troponin-I using LDH assay kit (Sigma-Aldrich, MO, USA) and Troponin I assay kit (Life Diagnostics, PA, USA), respectively. Coronary

effluents were analyzed for LDH levels (Sigma-Aldrich). Pyridine nucleotide ratios; $NADH/NAD^+$ and $NADPH/NADP^+$ were determined in frozen tissues using commercially available EnzyChrome $NAD^+$/NADH or $NADP^+$/NADPH kits (Bioassays, Hayward, CA).

### Protein expression analysis

Protein lysates from the LV of hyperoxia or normoxia exposed mice were prepared using T-PER reagent (Thermo scientific Inc, Waltham, MA). Utilizing Western blot, protein abundance of potassium channel genes of cardiac repolarization significance, Kv1.5 and pyridine nucleotide dependent metabolic regulator, SiRT1 was assessed as reported earlier (32).

### Quantitative real-time PCR

Total RNA was isolated from the left ventricle (LV) of hyperoxia or normoxia exposed mice using the Exiqon miRCURY RNA Isolation kit (Exiqon, Woburn, MA) and qRT-PCR analysis was performed as described previously (33) for potassium Kv subunit isoforms; Kvβ1.1, Kvβ1.2, Kvβ2.1 and Kvβ3.1, Nicotinamide Nucleotide Transhydrogenase (NNT), Nicotinamide phosphoribosyltransferase (Nampt) and Glucose-6-phosphate-dehydrogenase (G6PD). Ribosomal 18s RNA was used as an endogenous reference gene.

### Cell culture and pharmacological inhibition of SiRT1

Neonatal rat ventricular cardiomyocytes (H9C2) were procured from ATCC (Manassas, VA, USA) and grown in standard DMEM medium supplemented with 10% FBS, penicillin and streptomycin antibiotics as reported previously (32). Cells grown to 70- 80% confluence in 6 well plates were exposed in triplicates to SiRT1 inhibitor; splitomicin (100 μm), or dimethyl sulfoxide, DMSO (control) for 24 h. Total RNA was extracted from the treated cells using RNeasy mini kit (Qiagen Inc, Valencia, CA, USA). Transcript expression of SiRT1 and Kv1.5 was assessed by qRT-PCR approach as previously reported. Ribosomal 18s RNA was used as endogenous reference gene.

### Statistical Analysis

A student's t-test was used to identify average mean differences between the two groups, and statistical significance was assigned when $p\text{-}value \leq 0.05$.

## Results

### Electrical impairment and arrhythmias in hyperoxia treated mouse hearts

Electrical changes associated with hyperoxia treatment in mice were examined by ECG. We observed arrhythmias characterized by missed beats and slower heart rate in hyperoxia treated mice when compared with normoxia (Figure 1 A–B). The overall shape of the ECG traces was significantly different in the hyperoxia treated group compared with normoxia. Significant changes included augmentation of, RR (186.2±10.6 *vs.* 146.4±6.1 ms), PR (46.8±3.1 *vs.* 39.3±1.6), QRS (10.8±0.6 *vs.* 8.5±0.2 ms), QTc (57.1±3.5 *vs.* 40±1.4 ms) and JT (13.4±2.1 *vs.* 7±0.5 ms), intervals (Figure 1 C–G). Together, this data suggest that

exposure of mice to high oxygen induces cardiac arrhythmias and significantly decreases repolarization reserve.

### Hyperoxia treatment alters cardiac APD

For evaluating the electrical activity, we examined the cardiac AP traces acquired from LV epicardial surface from Langendorff perfused hearts. As shown in Figure 2A, the AP traces from normoxia group showed discrete waveform characteristic of normal cardiac electrical activity. In the hyperoxia treated mouse hearts, AP traces showed dome shaped prolongation indicating an altered repolarization reserve compared with normoxia hearts (Figure 2B). Although the *ex vivo* heart rate of hyperoxia exposed mice was lower than normoxia, the differences did not reach statistical significance (Figure 2C). Further, as shown in Figure 2D–E the APD values were significantly ($p \leq 0.05$) prolonged at various levels of repolarization (ms) including $APD_{10}$ (19.3±2 *vs.* 12.3±0.7), $APD_{30}$ (26±3.2 *vs.* 14.5±0.6), $APD_{50}$ (35.5±4 *vs.* 17.4±0.8), $APD_{70}$ (50±5.5 *vs.* 24.7±2.5), and $APD_{90}$ (73.8±9.5 *vs.* 50.9±3.1) in the hyperoxia hearts when compared with normoxia. Prolongation of AP data in hyperoxia treated mice suggests a significant altered repolarization reserve.

### Elevation of serum markers in hyperoxia treated hearts

To identify the extent of cardiac injury in hyperoxia exposed mice, we estimated the serum levels of Cardiac troponin I (TnI) and LDH. The ELISA data showed that the cTnI levels were 4-fold higher ($p \leq 0.05$) in hyperoxia treated mice (1.2±0.35) compared with normoxia group (0.31±0.1), suggesting severe damage to the cardiac tissue (Figure 3A). As shown in Figure 3B, LDH release in hyperoxia group (5±0.29) was 1.4 fold higher ($p \leq 0.05$) compared with normoxia (3.5±0.24). Collectively, the biochemical data clearly suggests that hyperoxia treatment augments cardiac injury in mice.

### Hyperoxia caused reduced body weight and lung injury

Hyperoxia exposure for 72h significantly reduced the body weight by 11.5%, in mice (Figure 4A). Previous studies showed that hyperoxia causes lung injury, and therefore we assessed the hallmarks of hyperoxia induced lung injury by measuring lung edema and BALF cell count. Hyperoxia treatment resulted in nearly 8 fold increase in the wet to dry weight ratio of the lung (Figure 4B), suggesting significant lung edema. Further, hyperoxia treatment induced a 10 fold increase in the total number of cells in BALF (Figure 4C), indicating severe inflammation in the lungs.

### Potassium channel and Kvβ-subunit expression

Voltage gated-potassium channels determine the repolarization reserve of cardiomyocytes. Hyperoxia treatment resulted in a significant reduction of oxygen-sensitive Kv1.5 potassium channel protein expression (Figure 5A and 5C) in the LV, suggesting that prolonged hyperoxia treatment reduces potassium currents and repolarization reserve in the heart. As Kvβ-subunits bind to and regulate the surface expression and activity of various Kv channels including Kv1.5, We measured and identified that hyperoxia treatment alters the mRNA expression of Kvβ-subunit isoforms; Kvβ1.1, Kvβ1.2, Kvβ2.1 and Kvβ3.1 (Figure 6A).

These data show that hyperoxia induced stress alters the expression of the Kv1.5 and Kvβ genes, which are of repolarization significance in the heart.

### Increased reductive stress in hyperoxia treated hearts

Pyridine nucleotides play a major role in relaying the influence of cellular oxygen on to metabolism and ion channel function including Kv1.5 (22). We therefore measured the reduced (NADH and NADPH) and oxidized ($NAD^+$ and $NADP^+$) pyridine nucleotide ratios from hyperoxia or normoxia treated mouse hearts. As shown in Figure 7, our data showed a significant elevation in the ratios of both NADH/$NAD^+$ (2.3 fold) and NADPH/$NADP^+$ (4.9 fold) in hyperoxia treated mouse hearts, suggesting elevated reductive stress (47). Simultaneously, protein expression of $NAD^+$ dependent SiRT1, showed a marked 1.4-fold reduction in the LV of hyperoxia treated mice compared to that of normoxia (Figure 5B & 5D), suggesting decreased SiRT1 activity. However, the mRNA expression of pyridine nucleotide processing genes such as Nampt, but not NNT, significantly increased (Figure 6B) suggesting compensatory upregulation of NAD salvaging pathways to sustain $NAD^+$ levels (1). Together, these results suggests that hyperoxia enhances reductive stress and reduces SiRT1 activity in heart, a scenario that supports aggravated cardiac injury and ion channel dysregulation (1).

### SiRT1 inhibition represses Kv1.5 expression

Both the decreased SiRT1 expression and elevated reductive stress in hyperoxia exposed hearts points toward SIRT1 inhibition, which supports cardiac injury and ion channel dysregulation (1). This raises the possibility that SiRT1 inhibition regulates the reduced cardiac expression of Kv1.5 in the hyperoxia exposed hearts. To test this, we treated H9C2 cells with SiRT1 inhibitor, splitomicin. Indeed, 48 h exposure of H9C2 cells to Splitomicin (100 μm) significantly reduced the mRNA expression of SiRT1 and Kv1.5 to nearly 58% and 49%, respectively, when compared with vehicle treated control group (Figure 8). These results suggests that downregulation of Kv1.5 expression in hyperoxia treated mice hearts may be caused by SiRT1 inhibition.

## Discussion

Cardiovascular complications of hyperoxia breathing includes bradycardia and altered hemodynamic parameters such as decreased stroke volume and cardiac output (20, 33, 39, 45). In the lung, it has been demonstrated that hyperoxia leads to inflammation, oxidative stress and injury (29). Three day exposure of mice to high oxygen levels leads to increase in LV size (33) We used this model to identify the cardiotoxic effects of hyperoxia and report that hyperoxia treatment causes significant electrical abnormalities along with slower heart rate, cardiac arrhythmias, increased QTc interval and prolonged APD. Biochemical analyses suggest that altered Kv1.5 and SiRT1 expression along with changes in pyridine nucleotide ratios; NAD(P)H/NAD(P), may at least in part underlie the cardiac arrhythmias and injury induced by hyperoxia treatment in mice.

ECG assessment showed significantly slower heart rate (sinus bradycardia) and multiple episodes of skipped beats (sinus pause) in all the hyperoxia treated mice compared to normal

ECG in normoxia group, indicating cardiac arrhythmia. It is plausible that altered parasympathetic and/or sympathetic tone may mediate these changes as both autonomic nervous system components regulate rhythm and heart rate (6). Indeed, augmented vagal tone (parasympathetic activation) and/or sympatholysis have been suggested to mediate hyperoxia induced hemodynamic changes (27, 39, 40). Importantly, hyperoxia treatment altered electrical indices of cardiac repolarization significance; QTc and JT intervals, which are key components of the ECG measurement of repolarization reserve (10). The increased QTc and JT interval in this study suggests defects in cardiac repolarization reserve in the hyperoxia treated mice (10, 46). These findings were further corroborated by higher APD values observed in the heart of hyperoxia treated mice when measured during *ex vivo* perfusion. Together, these findings clearly show that the hypertrophic changes induced by hyperoxia alter the repolarization reserve of the heart. As reported before (33), we identified a decrease in cardiac output ($p < 0.05$), ejection fraction and fractional shortening (not significant), along with significant increase in left ventricular mass index measured by using echocardiography (Fig. S1). Therefore, these functional data support hyperoxia induced cardiac arrhythmias and functional impairment.

A major determinant of repolarization reserve and action potential duration in heart is the Kv channel complement of the myocardium (31). Cardiac expression of Kv4.2 and its auxiliary subunit KChIP2 that together regulate $I_{to,f}$ currents (3, 24) were shown to decrease upon hyperoxia treatment (33). The deficiency of Kv4.2 (3) or KChIP2 (24) in mice eliminates $I_{to,f}$ in ventricular cardiac myocytes and results in prolonged QT interval and elevated ST segments, respectively. It has been suggested that the rapid repolarization accomplished by $I_{to,f}$ currents in ventricles supports the high resting heart rate in mice (31). In this study, we showed decreased expression of Kv1.5 (a molecular correlate of $I_{k,\ slow1}$ currents) in the hyperoxia treated mouse hearts. The slowly inactivating potassium channel, Kv1.5 is also an important determinant of APD in the ventricular myocytes (14, 38), and decreased expression of Kv1.5 is expected to reduce the cardiac repolarization reserve. Previous studies demonstrate that both Kv4.2 and Kv1.5 are sensitive to oxygen levels (35, 37). Additionally, the activity and expression of these Kv channels in the heart is regulated by Kvβ subunits (14, 38, 41). Therefore, hyperoxia induces significant alterations of Kv channel expression that may lead to cardiac arrhythmia in mice.

The heart is highly sensitive to oxygen (30), and hyperoxia treated mice hearts undergo systemic hypoxia due to accumulation of lung fluid (23). It is likely that this may reduce cellular oxygenation, tissue metabolism and lead to elevated redox stress as observed through modified pyridine nucleotide levels. The increase in the amount of reduced pyridine nucleotides (NADH/NADPH) in the cell causes reductive stress (47). This likely modulates potassium channel function as the cytosolic components of voltage gated potassium channel β-subunits (Kvβ1–3) interact with pyridine nucleotides. The extent and the nature of these interactions vary depending on the intracellular concentrations of all four pyridine nucleotides [(NAD(P)H, NAD(H)], *in vivo* (22), and affect Kv channel gating and kinetics (42). Reduced pyridine nucleotides support Kv inactivation *via* Kvβ1 and 3, whereas oxidized pyridine nucleotides abolish inactivation caused by Kvβ subunits (22). Based on the overall changes noted in the present study, the increased availability of reduced pyridine

nucleotides and Kvβ subunit levels in hyperoxia state would likely cause increase in binding of NAD(P)H to Kvβ subunits and may alter Kv channel gating. In addition reduced expression of $NAD^+$ dependent transcriptional co-suppressor SiRT1 in hyperoxia treated mice hearts was also observed in the present study. SiRT1 regulates wide range of cellular processes including cell survival, apoptosis, cell growth and metabolism, and deacetylation of histones and non-histone proteins (13). Studies also showed that the mice defective of SiRT1 exhibit severe developmental defects in the heart and did not survive into post-natal stage (9, 28). Further, the optimal SiRT1 expression is deemed anti-hypertrophic and cardio-protective, and studies show that cardiac specific deletion of SiRT1 aggravates I/R injury in mice hearts (1, 21). Concomitant reduction of Kv1.5 and SiRT1 expression in both hyperoxia exposed hearts and SiRT1 inhibited H9C2 cells explain at least in part the hyperoxia induced Kv1.5 downregulation (Figure 7 and Figure S2). Decrease in SiRT1 in hyperoxia hearts may be due to the elevation of $NADH/NAD^+$ ratio, which activates CtBP-HIC1 mediated repression of SiRT1 (49). Given that prolonged hyperoxia treatment enhances redox stress in various tissues including the heart (2, 5, 7, 34), and that reduced pyridine nucleotides promote reactive oxygen species in an injured myocardium (17, 43), our data point to a potential mechanistic basis for the cardiotoxic effects of hyperoxia treatment observed in this study.

Previous research showed that hyperoxia treatment results in reduced body weight in rodents (12, 18, 19). We have confirmed these findings in both our previous (33) and the current study. Although we did not measure the food intake, decreased cellular energy supply is a likely contributor of body weight loss, as concomitant enteral nutrition attenuates hyperoxia induced weight loss in rats (12). Also, several studies showed that hyperoxia exposure results in significant lung injury, as featured by elevated oxidative stress, inflammation, alveolar damage and pulmonary edema (12, 15, 23, 29). A recent study showed that hyperoxia exposure adversely affect cellular pathways of aerobic and anaerobic metabolism in lung tissue decreasing energy availability (11). In line with these observations, an earlier study showed that enteral nutritional support of rats under hyperoxia treatment alleviates lung edema through preserved expression of important proteins (12). Collectively, it is plausible that the altered energy metabolism and the ensuing perturbations in cellular repertoire required for maintaining optimal organ structure and function may at least in part underscore the body weight loss and other deleterious effects of hyperoxia.

In conclusion, we show that hyperoxia treatment of mice leads to: 1) cardiac arrhythmia and decreased repolarization reserve, 2) elevated myocardial damage, 3) altered ratios of pyridine nucleotides and 4) decreased SiRT1 and Kv1.5 channel expression along with altered redox regulatory gene expression. Our study offers novel insights into the cardiotoxicity and ensued electrophysiological consequences caused by exposure to high levels of oxygen.

## Supplementary Material

Refer to Web version on PubMed Central for supplementary material.

## Acknowledgments

**Funding**: This work was supported by National Institutes of Health HL-102171, USF College of Pharmacy startup and seed grant to SMT, NIH R01-HL-105932 to NK.

## References

1. Abdellatif M. Sirtuins and Pyridine Nucleotides. Circulation Research. 2012; 111:642–656. [PubMed: 22904043]
2. Amicarelli F, Ragnelli AM, Aimola P, Bonfigli A, Colafarina S, Di Ilio C, Miranda M. Agedependent ultrastructural alterations and biochemical response of rat skeletal muscle after hypoxic or hyperoxic treatments. Biochimica et Biophysica Acta (BBA) - Molecular Basis of Disease. 1999; 1453:105–114.
3. Barry DM, Xu H, Schuessler RB, Nerbonne JM. Functional Knockout of the Transient Outward Current, Long-QT Syndrome, and Cardiac Remodeling in Mice Expressing a Dominant-Negative Kv4 Subunit. Circulation research. 1998; 83:560–567. [PubMed: 9734479]
4. Berul CI, Aronovitz MJ, Wang PJ, Mendelsohn ME. In Vivo Cardiac Electrophysiology Studies in the Mouse. Circulation. 1996; 94:2641–2648. [PubMed: 8921812]
5. Bin-Jaliah I, Dallak M, Haffor AS. Effect of hyperoxia on the ultrastructural pathology of alveolar epithelium in relation to glutathione peroxidase, lactate dehydrogenase activities, and free radical production in rats, Rattus norvigicus. Ultrastruct Pathol. 2009; 33:112–122. [PubMed: 19479651]
6. Boyett MR, Honjo H, Kodama I. The sinoatrial node, a heterogeneous pacemaker structure. Cardiovascular research. 2000; 47:658–687. [PubMed: 10974216]
7. Brueckl C, Kaestle S, Kerem A, Habazettl H, Krombach F, Kuppe H, Kuebler WM. Hyperoxia-Induced Reactive Oxygen Species Formation in Pulmonary Capillary Endothelial Cells In Situ. Am J Respir Cell Mol Biol. 2006; 34:453–463. [PubMed: 16357365]
8. Ceconi C, Bernocchi P, Boraso A, Cargnoni A, Pepi P, Curello S, Ferrari R. New insights on myocardial pyridine nucleotides and thiol redox state in ischemia and reperfusion damage. Cardiovasc Res. 2000; 47:586–594. [PubMed: 10963731]
9. Cheng HL, Mostoslavsky R, Saito S, Manis JP, Gu Y, Patel P, Bronson R, Appella E, Alt FW, Chua KF. Developmental defects and p53 hyperacetylation in Sir2 homolog (SIRT1)-deficient mice. Proc Natl Acad Sci U S A. 2003; 100:10794–10799. [PubMed: 12960381]
10. Crow RS, Hannan PJ, Folsom AR. Prognostic Significance of Corrected QT and Corrected JT Interval for Incident Coronary Heart Disease in a General Population Sample Stratified by Presence or Absence of Wide QRS Complex: The ARIC Study With 13 Years of Follow-Up. Circulation. 2003; 108:1985–1989. [PubMed: 14517173]
11. Das KC. Hyperoxia decreases glycolytic capacity, glycolytic reserve and oxidative phosphorylation in MLE-12 cells and inhibits complex I and II function, but not complex IV in isolated mouse lung mitochondria. PLoS One. 2013; 8
12. Factor P, Ridge K, Alverdy J, Sznajder JI. Continuous enteral nutrition attenuates pulmonary edema in rats exposed to 100% oxygen. J Appl Physiol (1985). 2000; 89:1759–1765. [PubMed: 11053323]
13. Finkel T, Deng CX, Mostoslavsky R. Recent progress in the biology and physiology of sirtuins. Nature. 2009; 460:587–591. [PubMed: 19641587]
14. Fiset C, Clark RB, Larsen TS, Giles WR. A rapidly activating sustained K+ current modulates repolarization and excitation-contraction coupling in adult mouse ventricle. J Physiol. 1997; 504(Pt 3):557–563. [PubMed: 9401964]
15. Fukumoto J, Fukumoto I, Parthasarathy PT, Cox R, Huynh B, Ramanathan GK, Venugopal RB, Allen-Gipson DS, Lockey RF, Kolliputi N. NLRP3 deletion protects from hyperoxia-induced acute lung injury. Am J Physiol Cell Physiol. 2013; 305:1.
16. Gole Y, Gargne O, Coulange M, Steinberg J-G, Bouhaddi M, Jammes Y, Regnard J, Boussuges A. Hyperoxia-induced alterations in cardiovascular function and autonomic control during return to normoxic breathing. Eur J Appl Physiol. 2011; 111:937–946. [PubMed: 21069379]

17. Gupte SA, Levine RJ, Gupte RS, Young ME, Lionetti V, Labinskyy V, Floyd BC, Ojaimi C, Bellomo M, Wolin MS, Recchia FA. Glucose-6-phosphate dehydrogenase-derived NADPH fuels superoxide production in the failing heart. J Mol Cell Cardiol. 2006; 41:340–349. [PubMed: 16828794]
18. He X, Zhao W. Cellular changes in bronchoalveolar lavage fluid in hyperoxia-induced lung injury. Front Med China. 2008; 2:370–373.
19. Hokuto I, Ikegami M, Yoshida M, Takeda K, Akira S, Perl A-KT, Hull WM, Wert SE, Whitsett JA. Stat-3 is required for pulmonary homeostasis during hyperoxia. J Clin Invest. 2004; 113:28–37. [PubMed: 14702106]
20. How OJ, Aasum E, Severson DL, Chan WY, Essop MF, Larsen TS. Increased myocardial oxygen consumption reduces cardiac efficiency in diabetic mice. Diabetes. 2006; 55:466–473. [PubMed: 16443782]
21. Hsu CP, Zhai P, Yamamoto T, Maejima Y, Matsushima S, Hariharan N, Shao D, Takagi H, Oka S, Sadoshima J. Silent information regulator 1 protects the heart from ischemia/reperfusion. Circulation. 2010; 122:2170–2182. [PubMed: 21060073]
22. Kilfoil PJ, Tipparaju SM, Barski OA, Bhatnagar A. Regulation of ion channels by pyridine nucleotides. Circ Res. 2013; 112:721–741. [PubMed: 23410881]
23. Kolliputi N, Shaik RS, Waxman AB. The inflammasome mediates hyperoxia-induced alveolar cell permeability. J Immunol. 2010; 184:5819–5826. [PubMed: 20375306]
24. Kuo HC, Cheng CF, Clark RB, Lin JJ, Lin JL, Hoshijima M, Nguyen-Tran VT, Gu Y, Ikeda Y, Chu PH, Ross J, Giles WR, Chien KR. A defect in the Kv channel-interacting protein 2 (KChIP2) gene leads to a complete loss of I(to) and confers susceptibility to ventricular tachycardia. Cell. 2001; 107:801–813. [PubMed: 11747815]
25. Lagishetty V, Parthasarathy PT, Phillips O, Fukumoto J, Cho Y, Fukumoto I, Bao H, Cox R Jr, Galam L, Lockey RF, Kolliputi N. Dysregulation of CLOCK gene expression in hyperoxia-induced lung injury. Am J Physiol Cell Physiol. 2014; 306:C999–C1007. [PubMed: 24696144]
26. Liu M, Sanyal S, Gao G, Gurung IS, Zhu X, Gaconnet G, Kerchner LJ, Shang LL, Huang CL-H, Grace A, London B, Dudley SC. Cardiac Na+ Current Regulation by Pyridine Nucleotides. Circ Res. 2009; 105:737–745. [PubMed: 19745168]
27. Lund, Kentala; Scheinin, Klossner; Helenius, Sariola H.; Jalonen. Heart rate variability in healthy volunteers during normobaric and hyperbaric hyperoxia. Acta Physiologica Scandinavica. 1999; 167:29–35. [PubMed: 10519974]
28. McBurney MW, Yang X, Jardine K, Hixon M, Boekelheide K, Webb JR, Lansdorp PM, Lemieux M. The mammalian SIR2alpha protein has a role in embryogenesis and gametogenesis. Mol Cell Biol. 2003; 23:38–54. [PubMed: 12482959]
29. Nagato AC, Bezerra FS, Lanzetti M, Lopes AA, Silva MA, Porto LC, Valenca SS. Time course of inflammation, oxidative stress and tissue damage induced by hyperoxia in mouse lungs. Int J Exp Pathol. 2012; 93:269–278. [PubMed: 22804763]
30. Neely JR, Rovetto MJ, Oram JF. Myocardial utilization of carbohydrate and lipids. Prog Cardiovasc Dis. 1972; 15:289–329. [PubMed: 4564017]
31. Nerbonne JM, Kass RS. Molecular physiology of cardiac repolarization. Physiol Rev. 2005; 85:1205–1253. [PubMed: 16183911]
32. Panguluri SK, Tur J, Chapalamadugu KC, Katnik C, Cuevas J, Tipparaju SM. MicroRNA-301a mediated regulation of Kv4.2 in diabetes: identification of key modulators. PLoS One. 2013; 8:3.
33. Panguluri SK, Tur J, Fukumoto J, Deng W, Sneed KB, Kolliputi N, Bennett ES, Tipparaju SM. Hyperoxia-induced hypertrophy and ion channel remodeling in left ventricle. Am J Physiol Heart Circ Physiol. 2013; 304:H1651–H1661. [PubMed: 23585127]
34. Pendyala S, Gorshkova IA, Usatyuk PV, He D, Pennathur A, Lambeth JD, Thannickal VJ, Natarajan V. Role of Nox4 and Nox2 in hyperoxia-induced reactive oxygen species generation and migration of human lung endothelial cells. Antioxid Redox Signal. 2009; 11:747–764. [PubMed: 18783311]
35. Perez-Garcia MT, Lopez-Lopez JR, Gonzalez C. Kvbeta1.2 subunit coexpression in HEK293 cells confers O2 sensitivity to kv4.2 but not to Shaker channels. J Gen Physiol. 1999; 113:897–907. [PubMed: 10352037]

36. Pillai JB, Isbatan A, Imai S, Gupta MP. Poly(ADP-ribose) polymerase-1-dependent cardiac myocyte cell death during heart failure is mediated by NAD+ depletion and reduced Sir2alpha deacetylase activity. J Biol Chem. 2005; 280:43121–43130. [PubMed: 16207712]
37. Pozeg ZI. In Vivo Gene Transfer of the O2-Sensitive Potassium Channel Kv1.5 Reduces Pulmonary Hypertension and Restores Hypoxic Pulmonary Vasoconstriction in Chronically Hypoxic Rats. Circulation. 2003; 107:2037–2044. [PubMed: 12695303]
38. Scheuermann-Freestone M, Madsen PL, Manners D, Blamire AM, Buckingham RE, Styles P, Radda GK, Neubauer S, Clarke K. Abnormal cardiac and skeletal muscle energy metabolism in patients with type 2 diabetes. Circulation. 2003; 107:3040–3046. [PubMed: 12810608]
39. Seals DR, Johnson DG, Fregosi RF. Hyperoxia lowers sympathetic activity at rest but not during exercise in humans. American Journal of Physiology - Regulatory, Integrative and Comparative Physiology. 1991; 260:R873–R878.
40. Shibata S, Iwasaki K, Ogawa Y, Kato J, Ogawa S. Cardiovascular neuroregulation during acute exposure to 40 – 70, and 100% oxygen at sea level. Aviat Space Environ Med. 2005; 76:1105–1110. [PubMed: 16370259]
41. Tipparaju SM, Li XP, Kilfoil PJ, Xue B, Uversky VN, Bhatnagar A, Barski OA. Interactions between the C-terminus of Kv1.5 and Kvbeta regulate pyridine nucleotide-dependent changes in channel gating. Pflugers Arch. 2012; 463:799–818. [PubMed: 22426702]
42. Tipparaju SM, Saxena N, Liu SQ, Kumar R, Bhatnagar A. Differential regulation of voltage-gated K+ channels by oxidized and reduced pyridine nucleotide coenzymes. American journal of physiology Cell physiology. 2005; 288:C366–C376. [PubMed: 15469953]
43. Ussher JR, Jaswal JS, Lopaschuk GD. Pyridine Nucleotide Regulation of Cardiac Intermediary Metabolism. Circ Res. 2012; 111:628–641. [PubMed: 22904042]
44. Visser YP, Walther FJ, Laghmani el H, Laarse A, Wagenaar GT. Apelin attenuates hyperoxic lung and heart injury in neonatal rats. Am J Respir Crit Care Med. 2010; 182:1239–1250. [PubMed: 20622042]
45. Waring WS, Thomson AJ, Adwani SH, Rosseel AJ, Potter JF, Webb DJ, Maxwell SR. Cardiovascular effects of acute oxygen administration in healthy adults. J Cardiovasc Pharmacol. 2003; 42:245–250. [PubMed: 12883329]
46. Yan G-X, Antzelevitch C. Cellular Basis for the Normal T Wave and the Electrocardiographic Manifestations of the Long-QT Syndrome. Circulation. 1998; 98:1928–1936. [PubMed: 9799215]
47. Yan L-J. Pathogenesis of Chronic Hyperglycemia: From Reductive Stress to Oxidative Stress. Journal of Diabetes Research. 2014; 2014:11.
48. Yee M, White RJ, Awad HA, Bates WA, McGrath-Morrow SA, O'Reilly MA. Neonatal hyperoxia causes pulmonary vascular disease and shortens life span in aging mice. The American journal of pathology. 2011; 178:2601–2610. [PubMed: 21550015]
49. Zhang Q, Wang SY, Fleuriel C, Leprince D, Rocheleau JV, Piston DW, Goodman RH. Metabolic regulation of SIRT1 transcription via a HIC1:CtBP corepressor complex. Proc Natl Acad Sci U S A. 2007; 104:829–833. [PubMed: 17213307]

## Highlights

- Hyperoxia treatment leads to arrhythmia with prolonged QTc and action potential duration.
- Hyperoxia treatment alters cardiac pyridine nucleotide [NAD(P)H/NAD(P)] levels.
- SiRT1 and Kv1.5 are co-regulated in hyperoxic heart injury.
- Hyperoxia may lead to cardiotoxicity.

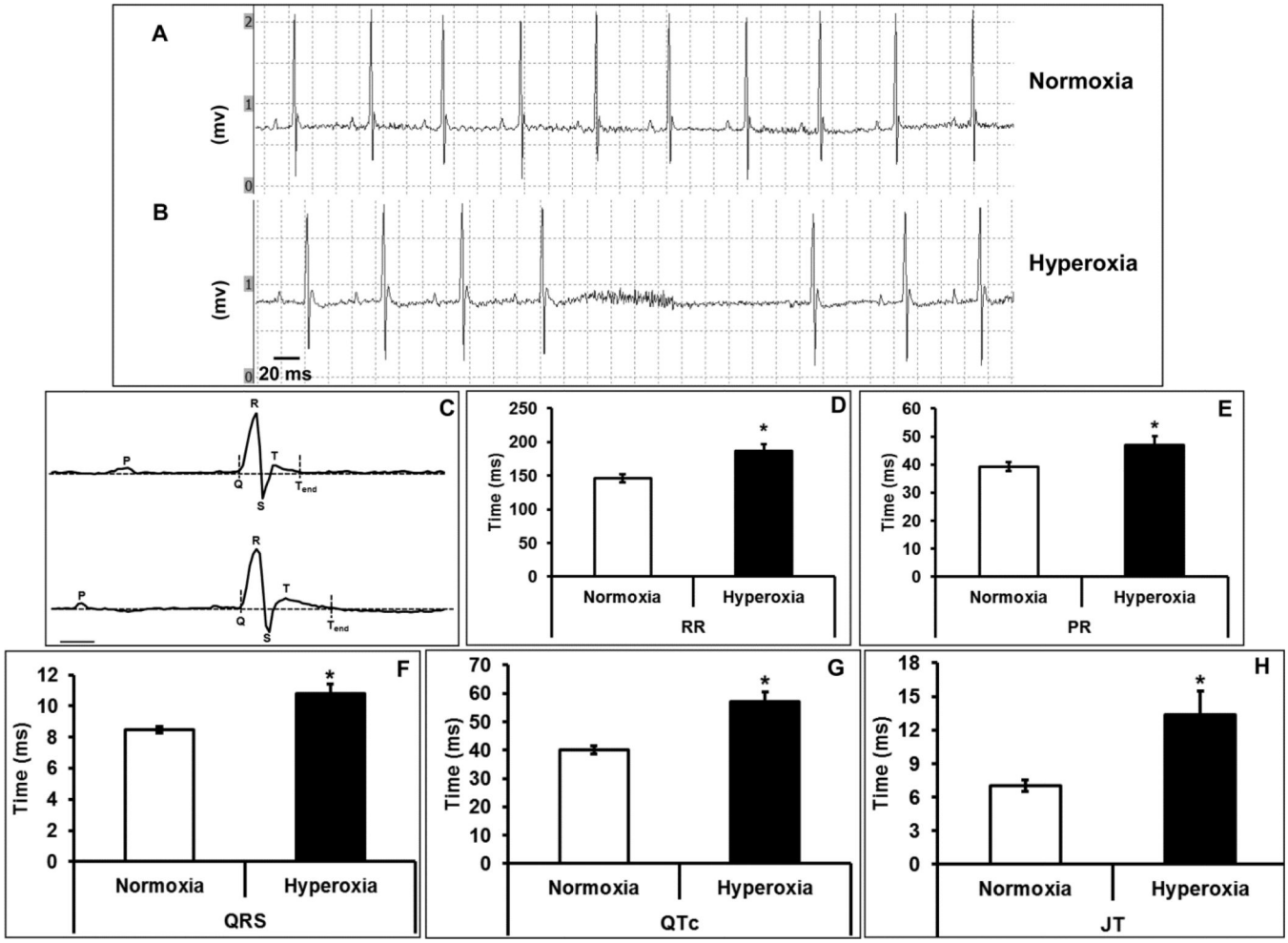


**Figure 1. Hyperoxia leads to cardiac conduction abnormalities**

Representative ECG (electrocardiogram) recording from normoxia (A) or hyperoxia (B) treated mice, C) analysis of ECG wave forms for normoxia and hyperoxia groups, D) RR interval, E) PR interval (F) QRS interval, (D) QTc interval and (E) JT interval. In the ECG chart recording, each division represents 20 ms on X-axis, and 0.5 mv on Y-axis (A and B). The scale bar denotes 10 ms for ECG recording in panel C. Bars represent mean time (ms) ± SEM of each group ($n=8$), *$p \leq 0.05$.

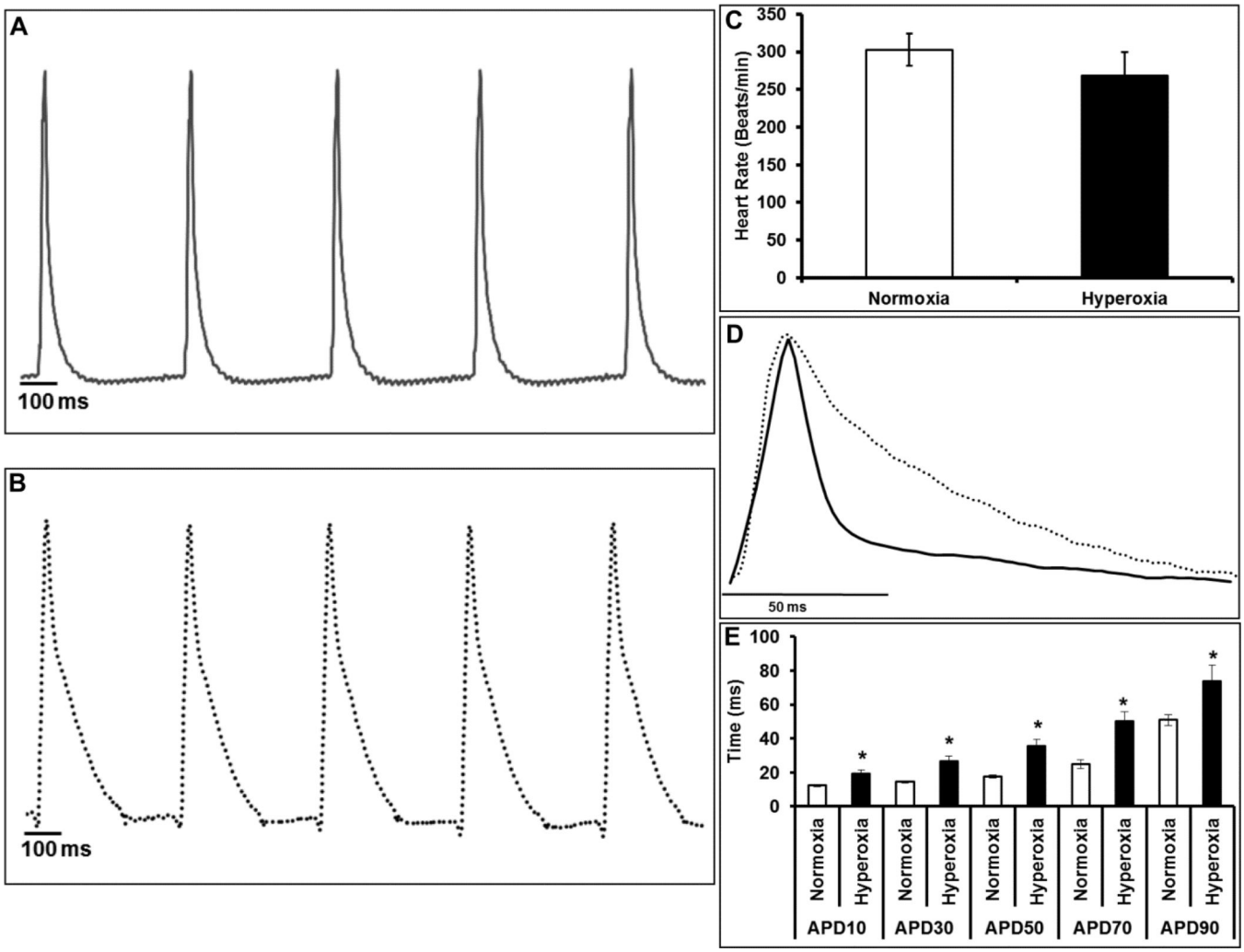


**Figure 2. Ventricular APD prolongation in hyperoxia exposed mice**

Representative traces of monophasic action potentials from (A) normoxia (solid line) or (B) hyperoxia (dotted line) exposed hearts. Heart rate (C), overlay of the normalized representative trace from normoxia (solid line) and hyperoxia (dotted line) groups showing a change in the action potential waveform and duration (APD) (D), graph plot for action potential durations at various levels of repolarization; APD 10, 30, 50 and 90 (E). Bars represent mean ± SEM of each group (*n=8*), *p ≤ 0.05 normoxia vs. hyperoxia. The peak amplitudes were normalized to 1 and overlaid to depict action potential changes.

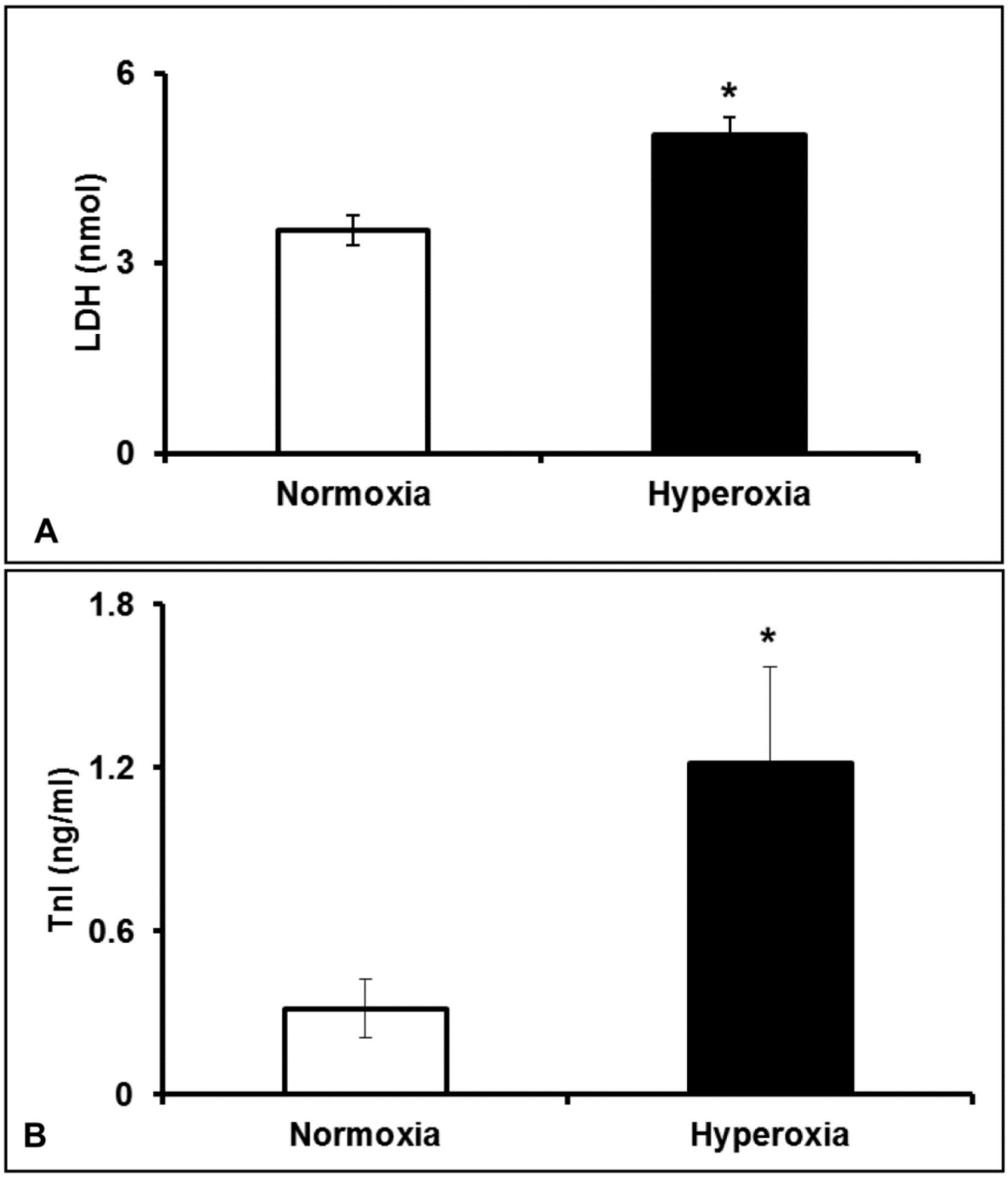


**Figure 3. Elevated serum markers of myocardial injury in hyperoxia treated mice**

Serum levels of Cardiac troponin I (TnI) (A) and LDH levels (B) in hyperoxia or normoxia exposed mice. Bars represent mean ± SEM of each group (*n=8*). Significant difference between the group averages was represented by an asterisk (*), $p \leq 0.05$.

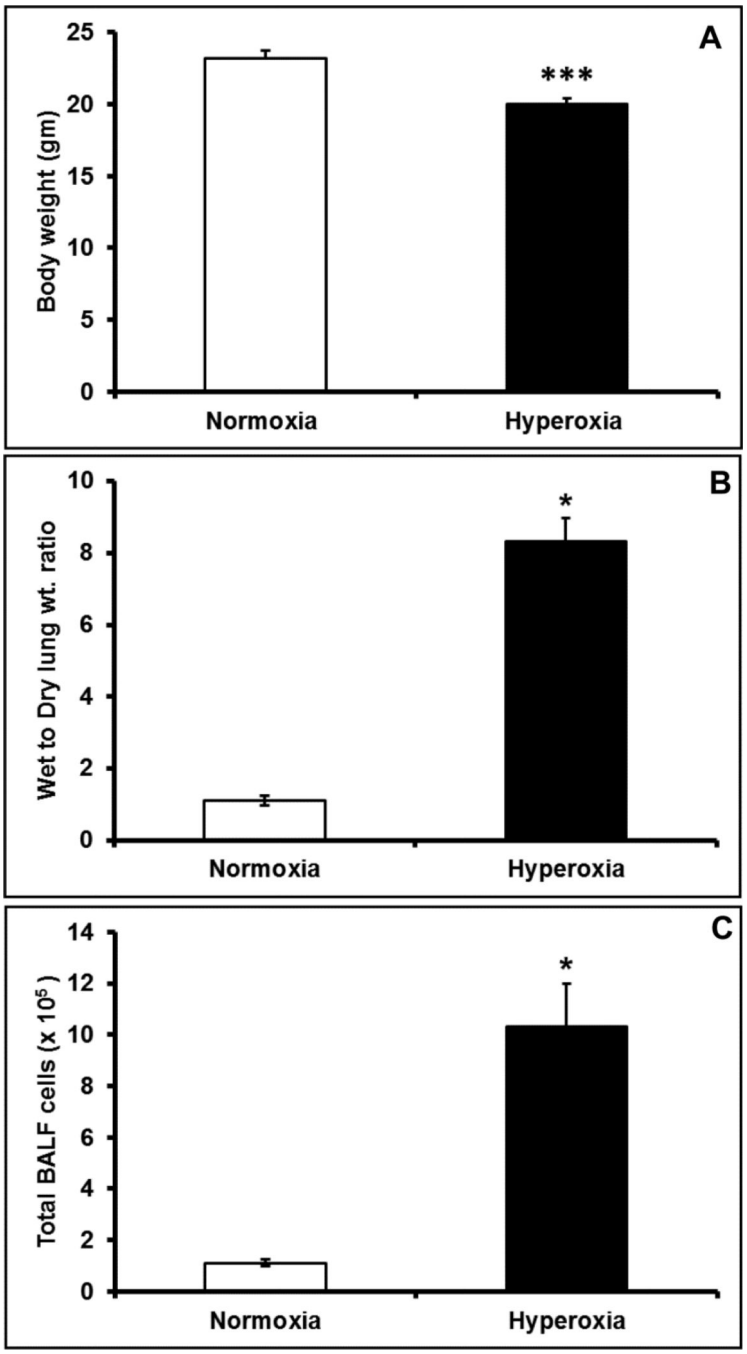


**Figure 4. Hyperoxia exposure resulted in decreased body weight and lung injury**

Hyperoxia or normoxia exposed mice were assessed for (A) body weight changes, (B) Lung edema measured as wet to dry weight ratio and (C) total inflammatory cell infiltration in bronchioalveolar lavage (BAL). Bars represent mean ± SEM, *n=6*. All comparisons were considered significant when $p \leq 0.05$, and represented by an asterisk (*).

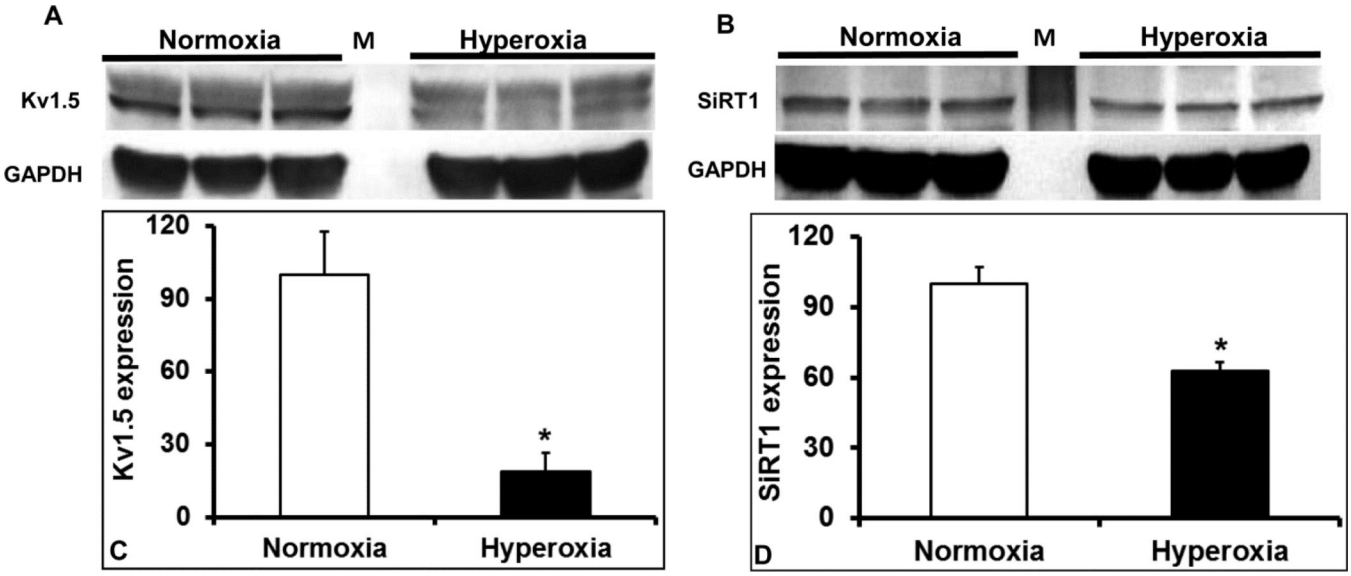


**Figure 5. Western blots of transcriptional mediators and ion channel proteins in hyperoxia exposed hearts**

Protein lysates of left ventricle of hyperoxia and normoxia exposed mice were assayed for changes in protein abundance of ion channel protein components, Kv1.5 (A) and transcription regulatory gene; SiRT1 (B). Densitometry values of each probed protein were normalized to GAPDH band of corresponding sample and reported as mean ± SEM (*n*=3) of normalized expression ratio of Kv1.5 (C) and SiRT1 (D). All comparisons were considered significant when $p \leq 0.05$ and represented by an asterisk (*).

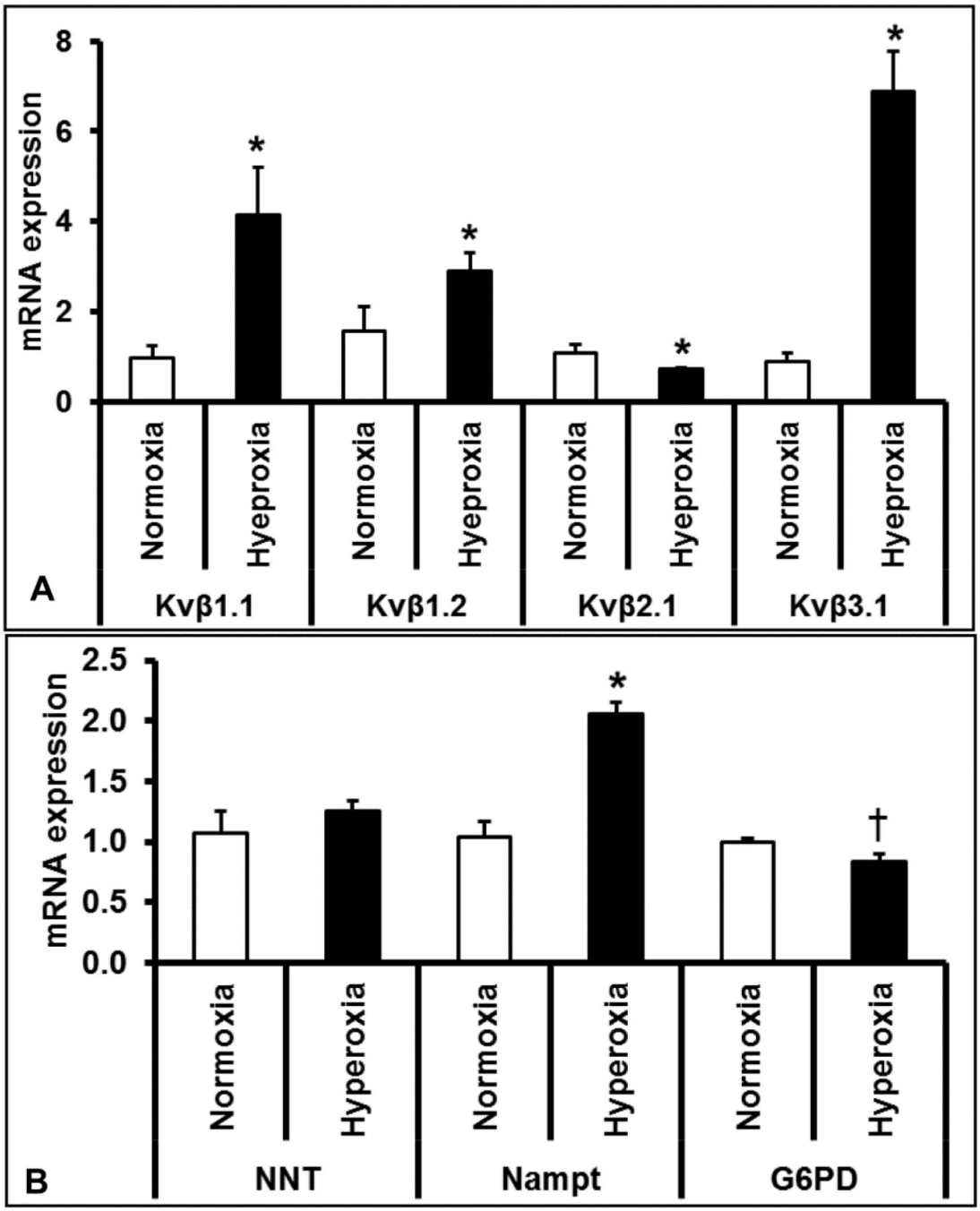


**Figure 6. Quantitative real-time PCR analysis of genes involved in pyridine nucleotide metabolism and Kv channel regulation**

Total mRNA extracted from the left ventricle of hyperoxia and normoxia exposed mice were analyzed for expression changes of potassium channel (Kv) β subunits Kvβ1.1, Kvβ1.2, Kvβ2 and Kvβ3 (A) and redox modulator genes such as nicotinamide nucleotide transhydrogenase (NNT), Nicotinamide phosphoribosyltransferase (Nampt) and Glucose-6-phosphate-dehydrogenase (G6PD) (B). Expression of ribosomal 18s RNA was used as an endogenous reference gene. Bars represent mean ± SEM of mRNA fold changes in

hyperoxia group as compared to normoxia group ($n=3$, $p < 0.05$). Significantly different groups were identified by an asterisk (*), and p=0.07 was indicated by a dagger (†).

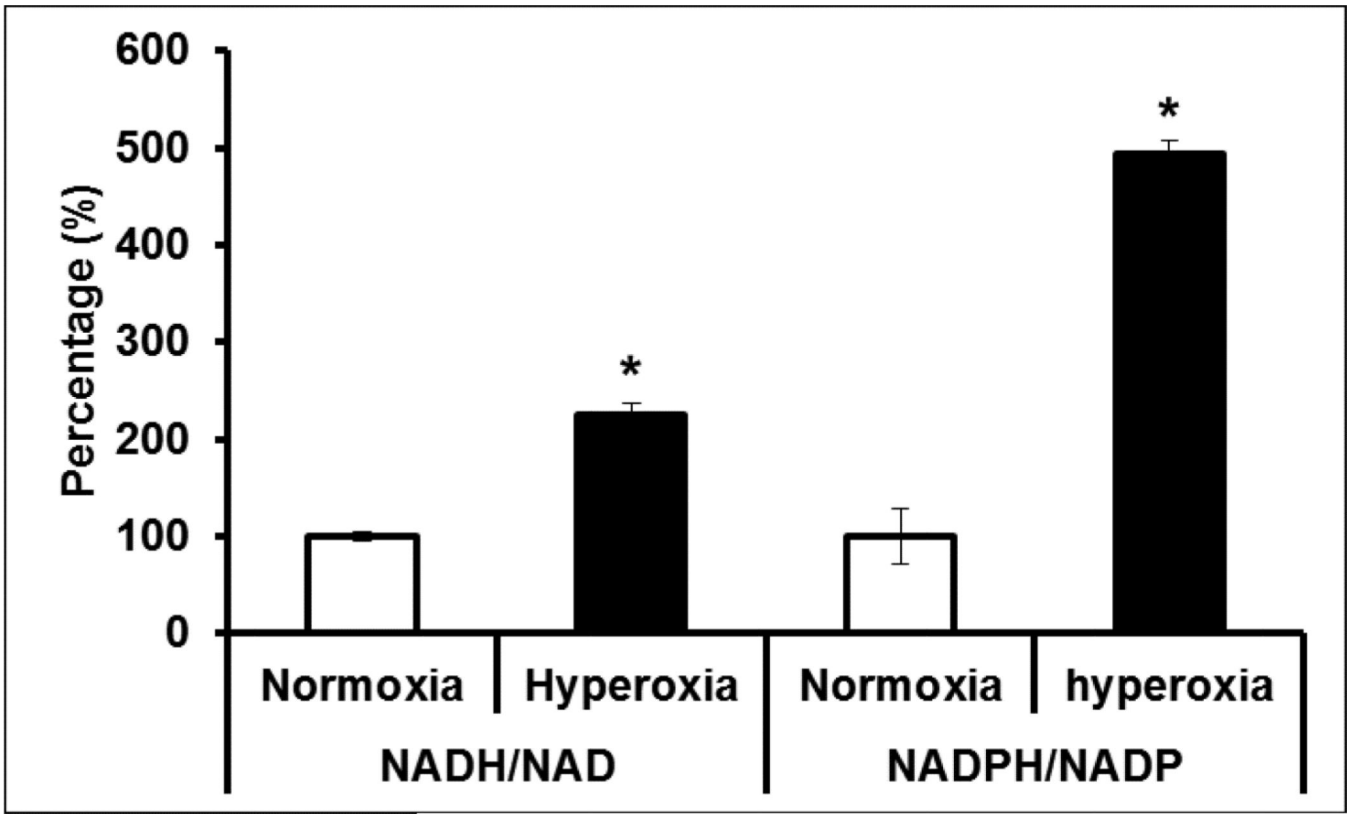


**Figure 7. Redox status of hyperoxia treated hearts**

Ratio of NADPH/NADP and NADH/NAD were measured from hyperoxia or normoxia treated mouse hearts and data presented as percentage. Bars represent mean (±SEM) of *n=6*, *p≤0.05.

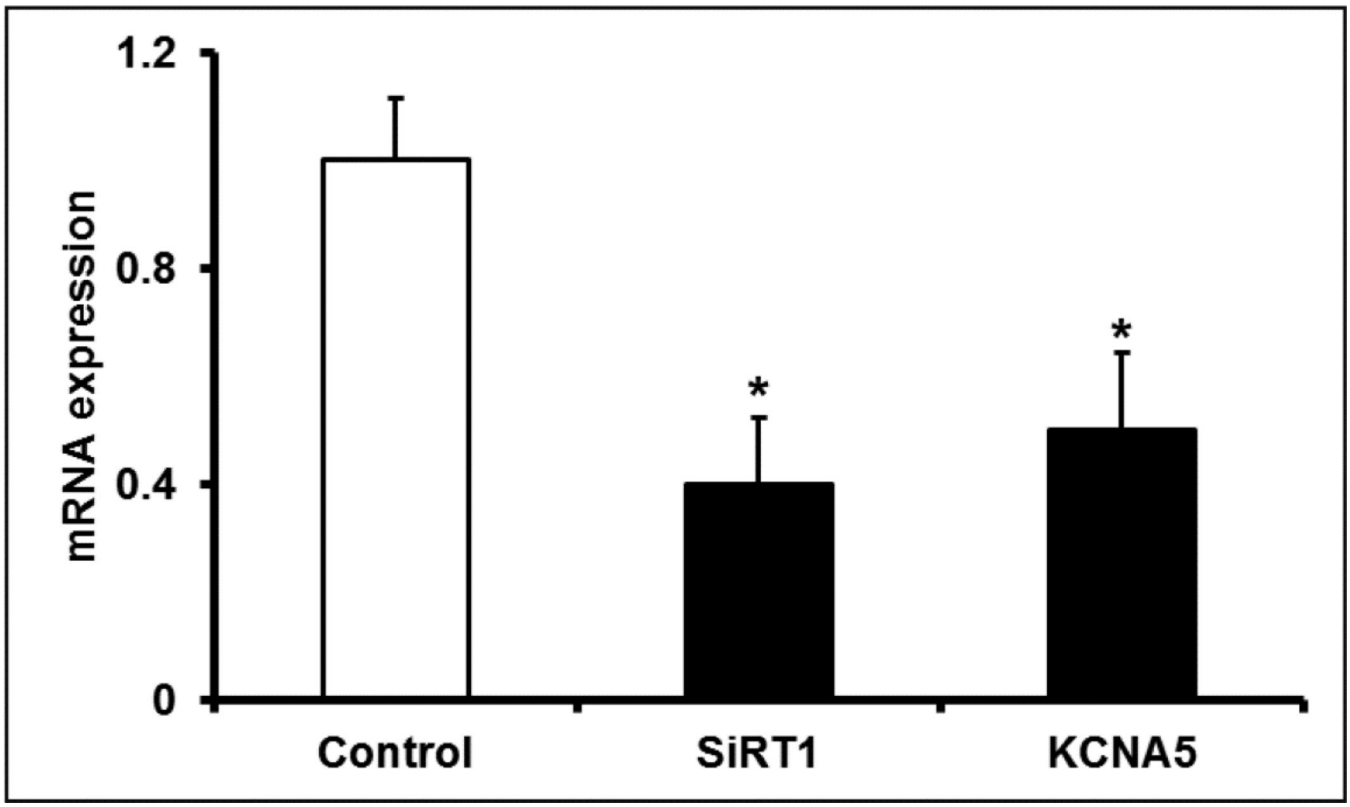


**Figure 8. SiRT1 inhibition downregulates Kv1.5**

H9C2 cells were treated for 48 h with SiRT1 inhibitor; Splitomicin (100 μM) or dimethyl sulfoxide, DMSO (control). RNA was extracted and SiRT1 and Kv1.5 mRNA expression was assessed by qRT-PCR. Ribosomal 18s RNA was used as an endogenous reference gene. Bars represent mean ± SEM (*n=3*), and * represents $p \leq 0.05$.

**Table 1**

Primers used in quantitative real-time PCR analysis

| Gene | Forward Primer | Reverse Primer |
|---|---|---|
| Kvβ1.1 | CAA AGC AGA CTG GCA TGA AA | TCC ACC CCA GTA GAG TTT GG |
| Kvβ1.2 | GAA TGG AAA TGC CTG GAG AA | GTG CGA CAG AGT AGG CTT CC |
| Kvβ2.1 | AGT CCC AAA AGA CAG CTC CA | CTT TTC CAG CAG CGT AGA CC |
| Kvβ3.1 | AAA CAG AGC GTG GCT TGA GT | CTT GTT GCT TCT TGC CTT CC |
| NNT | TGT CTC CTG CGG GGG TCC AG | GAA GCT TCG CCT GCG CCT GA |
| Nampt | TCC CCA GAG GGA ACG TGC TGT | GCC CCT ATG CCA GCA GTC TCT T |
| G6PD | TAG ATG CGG AAG GTC GGG CCA | GCG CAC CTG TCC GCT GTA GG |
| 18s | ACC TGG TTG ATC CTG CCA GTA G | TTA ATG AGC CAT TCG CAG TTT C |

Kvβ: Voltage gated potassium channel β-subunit, NNT: nicotinamide nucleotide transhydrogenase, Nampt: Nicotinamide phosphoribosyltransferase, G6PD: Glucose-6-phosphate-dehydrogenase, 18S: ribosomal RNA